

Ray-tracing and Interferometry in Schwarzschild Geometry

Sina Khorasani, Farhad Karimi

School of Electrical Engineering, Sharif University of Technology, Tehran, Iran

khorasani@sina.sharif.edu

Abstract

In a recent paper, we have discussed how the equivalent medium of Schwarzschild metric gives rise to an optically anisotropic description of space. Here, we show by direct numerical integration of ray-tracing equations, that the images of gravitational lensing due to a spherical blackhole in the Einstein's isotropic medium and Schwarzschild's anisotropic medium look almost the same, except with regard to the apparent size. We conclude that interpretation of gravitational lensing based on Einstein's isotropic medium over-estimates the mass of blackhole, up to an appreciable extent, compared to the Schwarzschild's anisotropic medium. We furthermore present a short discussion on the possibility of interferometric detection of static gravity.

1. Introduction

Light propagation in gravitational fields [1] has been a matter of intense research during the past decades. Recent experiments of general relativity using the weak gravitational lensing data [2] has revealed that alternative theories of gravity are not excluded. Progress in single atom optics has enabled an accurate tabletop experimental verification of the red shift [3]. Also, advances in the field of artificial metamaterials has established a bridge between the general relativity and optics of anisotropic media [4,5] through the equivalent medium theory [6,7]. This has been newly used to perform microscopic scale tests of propagation under the influence of gravity [8]. An extensive review of the theory and applications of transformation optics has just been published [9].

Recently, a detailed and exact theory of the propagation in the curved space, and in particular, for the Schwarzschild metric has been published by the author [10]. It was shown that the Schwarzschild metric is accompanied by an anisotropy, which inevitably gives rise to an optically anisotropic space. Correction to the Einstein's expression for light deflection was shown and ray-tracing equations were derived. We showed that the time-reversal symmetry of Maxwell's equations breaks down for rotating spacetimes, and through the equivalence principle, we concluded that the light speed should be no longer isotropic for non-inertial frames [10]. Moreover, we had provided some evidence [11], that the anisotropic light propagation in Schwarzschild geometry agrees to Virbhadra's expression [12], by direct calculation of deflection angle in the equivalent medium.

Here, we present simulated images of gravitational lensing by ray-tracing of light beams in both the Einstein's isotropic and Schwarzschild's anisotropic mediums. As it will be shown, the expected anisotropy of space does not affect the appearance of the images, but their apparent sizes. In this way, we establish that the analysis of Einstein's formulation of light deflection actually over-estimates the true mass of blackholes.

Another conclusion drawn from the possible anisotropy of space, as it will be discussed, is the possibility of optical detection of gravity beyond geometrical optics [13]. We also explicitly compare Schwarzschild and gravitational wave metrics, and show that the former is stronger by many orders of magnitude. Hence, we will argue that in principle it would be possible to reveal the existence of a Schwarzschild geometry through a local optical interferometry. For this purpose, the interferometer arms need to rotate by at least 90° in a plane passing through the center of the massive body.

2. Curved Spacetime Metrics

Here, we only discuss Newtonian and Schwarzschild metrics briefly. The first is given by

$$ds^2 = -c^2 \left(1 - 2 \frac{r_s}{r} \right) dt^2 + (dx^2 + dy^2 + dz^2) \quad (1)$$

where $r_s = 2GM / c^2$ is the Schwarzschild radius of the star with M and G respectively being its mass and gravitational constant, and $dl^2 = dx^2 + dy^2 + dz^2$ is the spacelike path element. Denoting the gravitational potential by $\Phi = -r_s / r$, the resulting refractive index is [10]

$$n = (1 + 2\Phi)^{-\frac{1}{2}} \quad (2)$$

In the limit of small $|\Phi| \approx 0$ or $r \gg r_s$, it becomes [14]

$$n \approx 1 - \Phi \quad (3)$$

This is the Einstein's 1911 early result. In contrast, the Schwarzschild metric is [15, p. 607]

$$ds^2 = -c^2 \left(1 - \frac{r_s}{r}\right) dt^2 + \frac{dr^2}{1 - \frac{r_s}{r}} + r^2 (d\theta^2 + \sin^2 \theta d\phi^2) \quad (4)$$

where (r, θ, ϕ) are the standard spherical coordinates. Unlike (1), the metric (4) is evidently anisotropic, in which the spacelike path element $dl^2 = dr^2 + r^2 (d\theta^2 + \sin^2 \theta d\phi^2)$ does not appear explicitly. The common practice is to transform (5) using the so-called isotropic coordinates [10,15], to obtain the well-known result

$$n \approx 1 - 2\Phi \quad (5)$$

Comparing to (3) reveals a correction factor of two [10,15]. But as we have already discussed in detail [10], isotropic coordinates rely on definition of a non-physical radial coordinate ρ defined by $r = \rho \left(1 + \frac{r_s}{2\rho}\right)^2$, which eventually disregards the physical anisotropy of (4). This normally could lead to physical implications, which are at best partially correct. Through an extensive direct algebraic analysis, however, it is possible [10] to show that the exact refractive index is

$$n = \left(\frac{r}{r_s}\right)^2 \left(\frac{r}{r_s} - 1\right)^{-\frac{3}{2}} \left(\frac{r}{r_s} - \sin^2 \psi\right)^{-\frac{1}{2}} \quad (6)$$

where the angle ψ is made by the radius r and wavevector \mathbf{k} . For small Φ , we get

$$n \approx 1 - \frac{3 + \sin^2 \psi}{2} \Phi \quad (7)$$

The correction factor in (5), hence actually varies between $3/2$ and 2 depending on the propagation angle. This anisotropy is present everywhere around a massive object, so that the maximum change in n by changing ψ could reach as high as $|\Phi|/2 = (GM/c^2)/r$. Based on the available estimates [15, p. 459] and for an experiment at Earth's distance from Sun, this figure is of the order of 10^{-8} , while it would be only about 6×10^{-10} at the surface of Earth when the gravity of Sun is neglected. We later argue that a local interferometry similar to the Laser Interferometer Gravitational wave Observatory (LIGO) could reveal the existence of Schwarzschild metric.

3. Ray-tracing Using Transformation Optics

3.1. Theory of Ray-tracing

The ray-tracing equations of Schwarzschild geometry in the equivalent medium read [10]

$$\begin{aligned} \frac{d}{dl} \mathbf{S} &\approx \begin{bmatrix} -(\hat{k} \cdot \hat{r}) \frac{\Phi}{r} & \frac{1 + (\hat{k} \cdot \hat{r})^2 \Phi}{k} \\ \frac{2 - \frac{3}{2}(\hat{k} \cdot \hat{r})^2}{r^2} k \Phi & \frac{\Phi}{r} (\hat{k} \cdot \hat{r}) \end{bmatrix} \mathbf{S} \\ &= \begin{bmatrix} 0 & \frac{1}{k} \\ 0 & 0 \end{bmatrix} \mathbf{S} + \Phi \begin{bmatrix} -\frac{\hat{k} \cdot \hat{r}}{r} & \frac{(\hat{k} \cdot \hat{r})^2}{k} \\ \frac{2 - \frac{3}{2}(\hat{k} \cdot \hat{r})^2}{r^2} k & \frac{\hat{k} \cdot \hat{r}}{r} \end{bmatrix} \mathbf{S} \end{aligned} \quad (8)$$

in which, $\hat{r} = \mathbf{r}/r$ is the unit radial vector measured from the origin of star, and $\hat{k} = \mathbf{k}/k$ is the unit propagation vector, and $\mathbf{S} = \begin{bmatrix} \mathbf{r} & \mathbf{k} \end{bmatrix}^T$. This equations may be easily integrated in 2D using

the initial conditions $\mathbf{r}(0) = -d\hat{y}$ and $\mathbf{k}(0) = k\hat{x}$, since the ray moves on the plane $(\mathbf{r}(0), \mathbf{k}(0))$. Clearly, the closest distance of approach is $d = r_0$.

Through an analysis similar to what is done in [10], it is fairly easy to show that the ray-tracing equations for the Einstein's isotropic medium simply are

$$\begin{aligned} \frac{d}{dl}\mathbf{S} &\approx \begin{bmatrix} 0 & \frac{1}{k} \\ \frac{2}{r^2}k\Phi & 0 \end{bmatrix}\mathbf{S} \\ &= \begin{bmatrix} 0 & \frac{1}{k} \\ 0 & 0 \end{bmatrix}\mathbf{S} + \Phi \begin{bmatrix} 0 & 0 \\ \frac{2}{r^2}k & 0 \end{bmatrix}\mathbf{S} \\ &= \frac{d}{dl}\mathbf{S}|_{\text{Isotropic}} \end{aligned} \tag{9}$$

It should be added that both (8) and (9) are correct to $O(\Phi)$. In the absence of gravitational field with $\Phi = 0$, both sets of ray-tracing equations relax to that of a straight light beam moving along \hat{k} . Therefore, any correction in ray trajectories due to the anisotropy of Schwarzschild's space arises from the term given by

$$\frac{d}{dl}\mathbf{S}|_{\text{Anisotropic}} \approx (\hat{k} \cdot \hat{r})\Phi \begin{bmatrix} -\frac{1}{r} & \frac{\hat{k} \cdot \hat{r}}{k} \\ -\frac{3(\hat{k} \cdot \hat{r})}{2r^2}k & \frac{1}{r} \end{bmatrix}\mathbf{S} \tag{10}$$

which is proportional to $(\hat{k} \cdot \hat{r})\Phi$. Here, $\frac{d}{dl}\mathbf{S}|_{\text{Total}} = \frac{d}{dl}\mathbf{S}|_{\text{Isotropic}} + \frac{d}{dl}\mathbf{S}|_{\text{Anisotropic}}$. This means in

other words that only at the closest distance of approach where $\hat{k} \perp \hat{r}$, the behavior of light rays in Einstein and Schwarzschild spaces are the same.

Hereby, we will perform integrations of both sets of ray-tracing equations and compare the results.

3.2. Results

Numerical integration of (8) and (9) needs an accurate integration scheme. We actually noted that simple Euler's integration scheme is far more than insufficient for this purpose. Hence, a fourth-order Runge-Kutta method was implemented to achieve stable and reliable results. Calculations were done using a code written in C++ language for maximal performance.

Light rays passing nearby a black hole are illustrated in Fig. 1. Since according to (8) and (9), light rays always lies on a single plane passing through blackhole's center, ray-tracing on a 2D plane is sufficient to notice the deflection of light rays. Fig. 1a shows the light trajectories due to the Einstein's isotropic medium, while Fig. 1b shows the same for the Schwarzschild's anisotropic medium. Calculated angles of deflection were noticed to be in rough agreement with Einstein's formula for the angle of light deflection [15], given by $\alpha \approx 2r_s/r_0$.

It could be seen that Einstein's isotropic medium causes stronger deflection of light rays. This may be easily understood by referring to (7), which shows that the true refractive index varies between $1 + \frac{3}{2}|\Phi|$ and $1 + 2|\Phi|$ in the Schwarzschild space, while it is always equal to $1 + 2|\Phi|$ for the Einstein's isotropic medium. In other words, the light beam feels a smaller average refractive index in the Schwarzschild space, and therefore undergoes less deflection.

We also have simulated the images of gravitational lensing caused by a blackhole located at the origin. We consider three cases: (i) the star is located on-axis and lying at the observation axis (which is the line passing through the observer and blackhole center), (ii) the star is located slightly off-axis yet having an overlap with the observation axis, and (iii) the star is located fully off-axis having no overlap with the observation axis. In all simulations, the spatial coordinates were normalized to the blackhole radius r_s , such that the blackhole's radius becomes unity. For simplicity, the star's radius is also taken as unity and is located within 5 unit distances of the blackhole center. The observation point is also at the distance of 5 units away from the blackhole center, on the opposite side.

- (i) Fig. 2: Blackhole is located at $(0,0,0)$, star is located at $(0,0,-5)$, and the observation point is at $(0,0,+5)$. Because of the rotational symmetry with respect to the z -axis, the image would be also centrosymmetric. This will be seen in the form of the so-called Einstein's ring. The ring forms in both isotropic (red) and anisotropic (blue) spaces, but the image caused by the Einstein's isotropic medium is about 18% larger than the actual image obtained in the Schwarzschild's anisotropic medium.
- (ii) Fig. 3: Blackhole is located at $(0,0,0)$, star is located at $(+0.5,0,-5)$, and the observation point is at $(0,0,+5)$. Since the star has a unit radius, it has intersection with the observation axis, which is the same as z -axis. The configuration has no rotational symmetry, and hence the image is not centrosymmetric. Still the ring is unbroken, but the intensity of light on the ring is not uniform. Furthermore, the center of image has moved slightly to the right. Again, the images of isotropic (red) and anisotropic (blue) spaces look the same in appearance, but the image of the Einstein's

isotropic medium is about 18% larger than that obtained in the Schwarzschild's anisotropic medium.

- (iii) Fig. 4: Blackhole is located at $(0,0,0)$, star is located at $(+1.5,0,-5)$, and the observation point is at $(0,0,+5)$. Since the star has a unit radius, it has no intersection with the observation axis, i.e. z -axis. Again, the configuration has no rotational symmetry, and hence the image is not centrosymmetric. But the Einstein's ring is broken into two unequal crescents. Also, the center of image has moved slightly to the right. Again, the images of isotropic (red) and anisotropic (blue) spaces look very similar, but the image of the Einstein's isotropic medium is about 18% larger than that of the Schwarzschild's anisotropic medium.

The results of ray-tracing are in agreement with the well-known images simulated in the literature [16,17]. In summary, the Einstein's isotropic medium due to (5) would significantly over-estimate the true deflection of light in Schwarzschild's anisotropic medium as given by (7).

4. Optical Interferometry

Now, in order to establish the connection between the gravity-induced optical anisotropy and gravitational waves, we take a look at the metric representing a gravitational wave [18]

$$ds^2 = (g_{ij} + \gamma_{ij})dx^i dx^j \quad (11)$$

where g_{ij} is the metric of the unperturbed geometry and γ_{ij} is the perturbation metric due to the gravitational wave. For a plane wave moving along x direction we have [18]

$$[\gamma_{ij}] = \begin{bmatrix} 0 & 0 & 0 & 0 \\ 0 & 0 & 0 & 0 \\ 0 & 0 & \gamma_{22} & \gamma_{23} \\ 0 & 0 & \gamma_{32} & \gamma_{33} \end{bmatrix} \quad (12)$$

where $\gamma_{22} = -\gamma_{33}$ and $\gamma_{23} = \gamma_{32}$. The two orthogonal polarizations are $\gamma_{22} \neq 0, \gamma_{23} = 0$ and $\gamma_{22} = 0, \gamma_{23} \neq 0$. Now, for simplicity we only take $\gamma_{22} = \delta, \gamma_{23} = 0$, to get [18]

$$ds^2 = -c^2 dt^2 + dx^2 + [1 + \delta \sin(Kx - \Omega t)] dy^2 + [1 - \delta \sin(Kx - \Omega t)] dz^2 \quad (13)$$

Here, Ω is the angular frequency of the gravitational wave, K is its wavenumber, and δ is its amplitude. The metric (14) is obviously anisotropic, and following [10] we obtain

$$n = (\mathbf{h} \cdot [\zeta] \cdot \mathbf{h} + \mathbf{h} \cdot [\rho] \cdot \mathbf{h})^{-\frac{1}{2}}, \text{ where } [\zeta] \text{ is the Minkowskian metric with } \mathbf{h} \cdot [\zeta] \cdot \mathbf{h} = 1, \text{ and } [\rho]$$

is due to the gravitational wave. If the amplitude of the wave is small, then binomial expansion

may be applied to get $n \approx 1 - \frac{1}{2} \mathbf{h} \cdot [\rho] \cdot \mathbf{h}$. Examining this result along y and z , respectively,

with $\mathbf{h} = \hat{y}$ and $\mathbf{h} = \hat{z}$, reveals that we must have $n_y \approx 1 - \frac{1}{2} \rho_{22} = 1 - \frac{1}{2} \delta \sin(Kx - \Omega t)$ and

$n_z \approx 1 - \frac{1}{2} \rho_{33} = 1 + \frac{1}{2} \delta \sin(Kx - \Omega t)$. At $x = 0$, this would be equivalent to an anisotropy of

$$\Delta n = n_y - n_z \approx \delta \sin(\Omega t) \quad (14)$$

which is expected to be of the order of 10^{-24} [18]; this is yet to be observed in LIGO.

As it can be seen, the fundamental operation of LIGO relies on the temporal geometrical anisotropy due to the passing gravitational field. Since Schwarzschild metric also causes such anisotropy, interferometry should be equally applicable to probe static gravitational fields. As stated above, the expected order of anisotropy caused by Sun is quite appreciable, being about 10^{-8} , which is at least 16 orders of magnitude stronger than that of typical gravitational waves.

This figure is large enough to be easily detectable on a tabletop setup. If it would, then most

normal optical setups had problems working on the Earth, due to interference with the gravity of Sun, Earth, and other massive objects nearby. This is clearly not the case, and as the matter of fact, nobody has noticed such a large deviation in interferometric experiments.

Classically, all experiments in search of optical anisotropy of space using optical interferometry (and other methods) have failed [19-27] to reveal the existence of any appreciable anisotropy. The proposal of OPTIS satellite [28] suggests a three-orders-of-magnitude improvement over earlier interferometric Michaelson-Morley experiments. What is notable in all the reported interferometric experiments is that they all used rotating optical tables, which had their planes of rotation in parallel to the surface of the Earth. This could result in observation of no change in refractive index as predicted by (7), and hence no gravity-induced anisotropy. For instance, in order to observe a change in refractive index due to gravity of the Earth, it would be necessary for the interferometer arms to rotate in a plane normal to the surface of the Earth. An interferometric experiment done as such, would rigorously establish the possibility of any gravity-induced optical anisotropy.

On the other hand, if interferometry fails to reveal the existence of Schwarzschild metric (which is the apparent case), then one could expect the gravitational waves not to be detectable, too. This might be able to explain why the LIGO experiment, despite its extremely high accuracy, has been unsuccessful in the search of gravitational waves.

5. Conclusions

Integration of ray-tracing equations obtained using transformation optics technique, has enabled us to compare the images of gravitational lensing in Einstein's isotropic and Schwarzschild's anisotropic media. It was established that anisotropy of Schwarzschild metric causes a first-order correction in terms of the gravitational potential, which causes a significant reduction in the apparent size of the image. This would mean that Einstein's expression for light deflection could significantly over-estimate the blackhole's mass. A discussion on the operation of optical interferometers in search of gravitational waves was presented, and it was pointed out that such experiments are all expected to detect the temporal anisotropy of spacetime caused by passing gravitational waves. Such anisotropy due to the gravities of the Sun and the Earth might already exist at the surface of the Earth, stronger by respectively sixteen and fourteen orders of magnitude. Hence, it was argued that optical interferometry might have been the inappropriate choice for detection of gravitational waves.

REFERENCES

- [1] W. P. Schleich, M. O. Scully, "General relativity and modern optics," in *New Trends in Atomic Physics*, R. Stora, G. Grynberg (eds.), *Proceedings of the Les Houches Summer School, Session XXXVIII, 1982*, (North Holland, Amsterdam, 1984).
- [2] R. Reyes, R. Mandelbaum, U. Seljak, T. Baldauf, J. E. Gunn, L. Lombriser, R. E. Smith, *Nature* 464 (2010) 256.
- [3] H. Müller, A. Peters, S. Chu, *Nature* 463 (2010) 926.
- [4] D. Schurig, J. B. Pendry, D. R. Smith, *Opt. Express* 14 (2006) 9794.
- [5] U. Leonhardt, T. G. Philbin, *Prog. Opt.* 53 (2009) 69.

- [6] I. E. Tamm, J. Russ. Phys. Chem. Soc. 56 (1924) 248.
- [7] J. Plebanski, Phys. Rev. 118 (1960) 1396.
- [8] D. A. Genov, S. Zhang, X. Zhang, Nature Phys. 5 (2009) 687.
- [9] H. Chen, C. T. Chan, and P. Sheng, Nature Mat. 9 (2010) 387.
- [10] S. Khorasani, B. Rashidian, Opt. Commun. 283 (2010) 1222.
- [11] S. Khorasani, Proc. SPIE 7597 (2010) 75971Y.
- [12] K. S. Virbhadra, Phys. Rev. D 79 (2009) 083004.
- [13] B. Mashhoon, Nature 250 (1974) 316.
- [14] A. Einstein, Ann. Phys. 35 (1911) 898.
- [15] C. W. Misner, K. Thorne, J. A. Wheeler, Gravitation (New York, W. H. Freeman and Company, 1973).
- [16] X.-H. Ye and Q. Lin, J. Mod. Opt. 55 (2008) 1119.
- [17] T. Müller and D. Weiskopf, Am. J. Phys. 78 (2010) 204.
- [18] Quarterly Progress Report, No. 105 (April 15, 1972), Research Laboratory of Electronics, Massachusetts Institute of Technology, Document LIGO-P720002-00-R.
- [19] J. P. Cedarholm, G. F. Bland, B. L. Havens, C. H. Townes, Phys. Rev. Lett 1 (1958) 342.
- [20] T. S. Jaseja, A. Javan, J. Murray, C. H. Townes, Phys. Rev. 133 (1964) A1221.
- [21] W. S. N. Trimmer, R. F. Baierlein, J. E. Faller, H. A. Hill, Phys. Rev. D 8 (1973) 3321.
- [22] A. Brillet, J. L. Hall, Phys. Rev. Lett. 42 (1979) 549.
- [23] J. D. Prestage, J. J. Bollinger, W. M. Itano, D. J. Wineland, Phys. Rev. Lett. 54 (1985) 2387.
- [24] E. Riis, L.-U. A. Andersen, N. Bjerre, O. Poulsen, S. A. Lee, J. L. Hall, Phys. Rev. Lett. 60 (1988) 81.

- [25] V V Ragul'skiĭ, Physics Uspekhi 40 (1997) 972.
- [26] H. Müller, S. Herrmann, C. Braxmaier, S. Schiller, and A. Peters, Phys. Rev. Lett. 91 (2003) 20401.
- [27] S. Schiller, P. Antonini, and M. Okhapkin, Lect. Notes Phys. 702 (2006) 401.
- [28] C. Lämmerzahl, H. Dittus, A. Peters, S. Schiller, Class. Quantum Grav. 18 (2001) 2499.

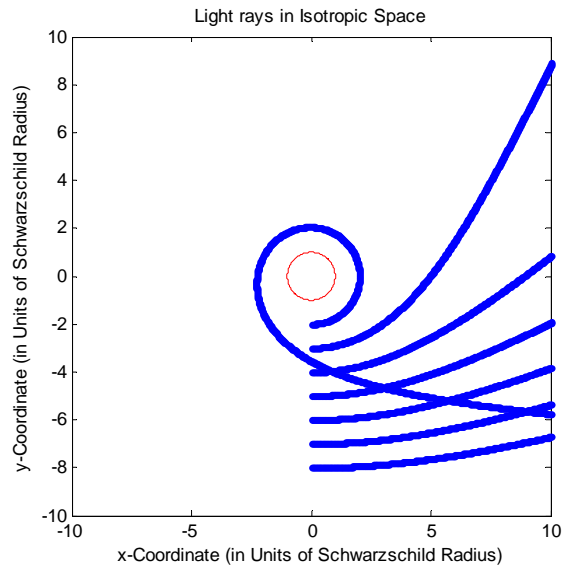
Figure Captions

Figure 1. Ray-tracing in space around a blackhole with radius r_s (shown as the red circle): (a) Einstein's isotropic medium; (b) Schwarzschild's anisotropic medium. Spatial dimensions are normalized to r_s .

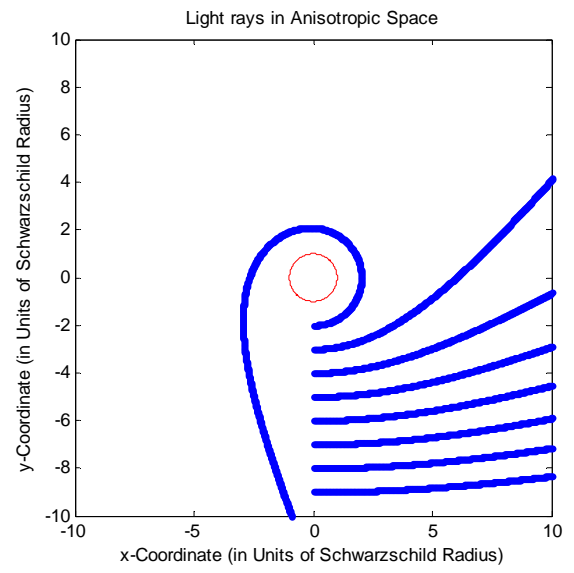
Figure 2. Einstein ring of an on-axis star with unit radius: (red) Einstein's isotropic medium; (blue) Schwarzschild's anisotropic medium. In both cases, the blackhole, star, and observer are located respectively at $(0,0,0)$, $(0,0,-5)$, and $(0,0,+5)$. Spatial dimensions are normalized to r_s .

Figure 3. Lensing image of an off-axis star with unit radius: (red) Einstein's isotropic medium; (blue) Schwarzschild's anisotropic medium. In both cases, the blackhole, star, and observer are located respectively at $(0,0,0)$, $(+0.5,0,-5)$, and $(0,0,+5)$. Spatial dimensions are normalized to r_s .

Figure 4. Lensing image of an off-axis star with unit radius: (red) Einstein's isotropic medium; (blue) Schwarzschild's anisotropic medium. In both cases, the blackhole, star, and observer are located respectively at $(0,0,0)$, $(+1.5,0,-5)$, and $(0,0,+5)$. Spatial dimensions are normalized to r_s .



(a)



(b)

Figure 1.

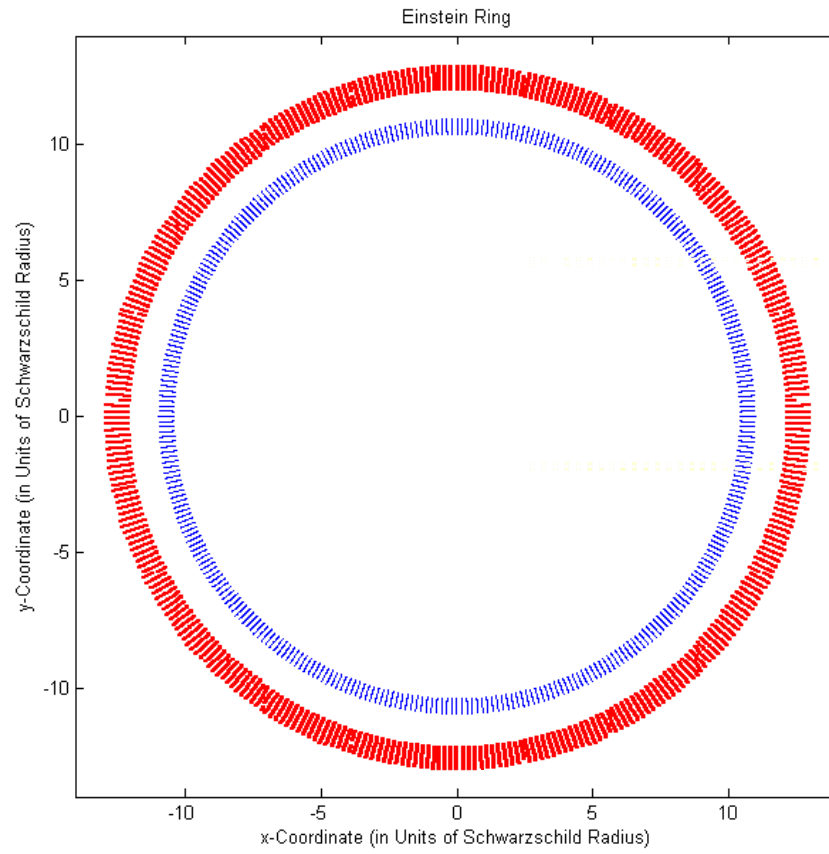


Figure 2.

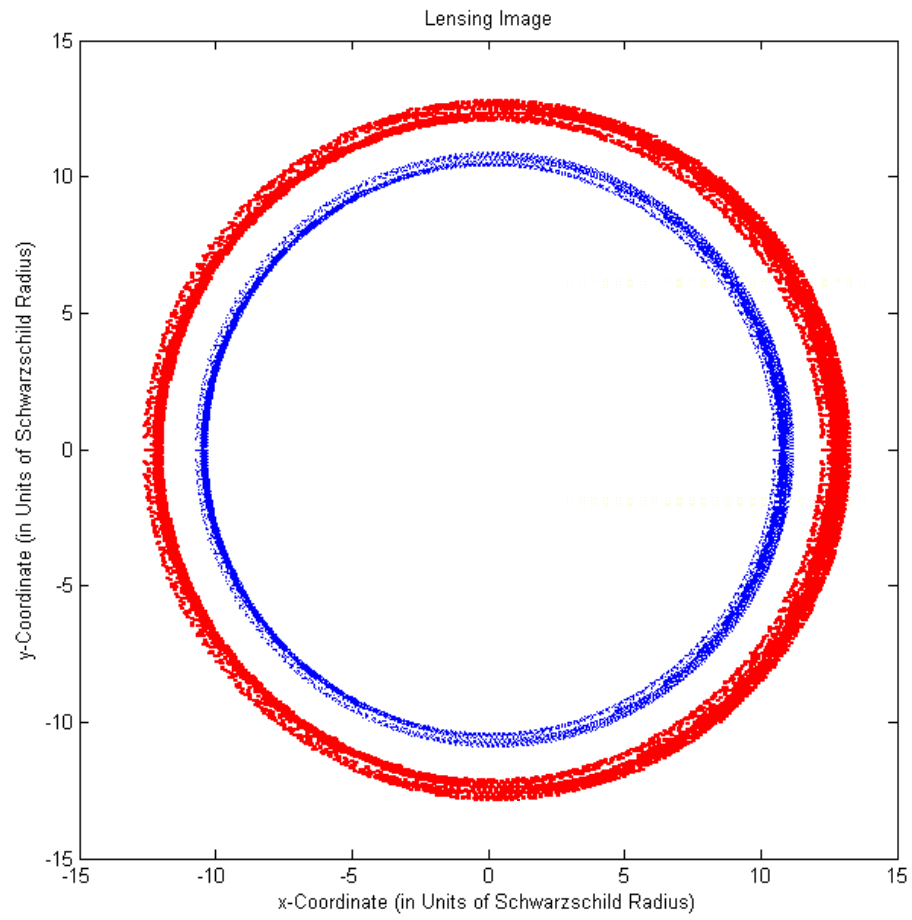


Figure 3.

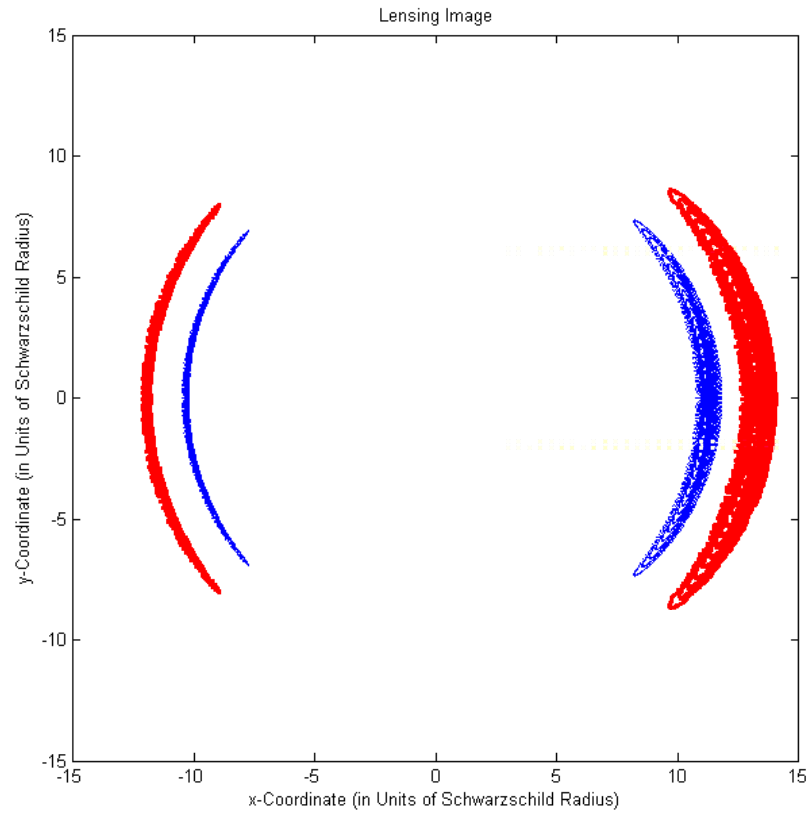


Figure 4.